Environmental Science & Technology

Article

pubs.acs.org/est

Effect of Groundwater–Lake Interactions on Arsenic Enrichment in Freshwater Beach Aquifers

Jacky Lee,[†] Clare Robinson,*[,†] and Raoul-Marie Couture[‡,§]

[†]Department of Civil and Environmental Engineering, Western University, London, Ontario N6A 5B9, Canada

[‡]Ecohydrology Group, University of Waterloo, Waterloo, Ontario N2L 3G2, Canada

[§]Norwegian Institute for Water Research, Gaustadalleen 21, NO-0575 Oslo, Norway

Supporting Information

ABSTRACT: Field measurements combined with numerical simulations provide insight into the water exchange, groundwater flow, and geochemical processes controlling the mobility of arsenic (As) in freshwater beach aquifers. Elevated dissolved As (up to 56 μg/L) was observed 1–2 m below the shoreline at two sandy beaches on Lake Erie, Ontario, Canada. Water and solid-phase analyses suggest that Fe (hydr)oxides present below the shoreline accumulate As, creating a risk of high As in the beach aquifer. Groundwater flow simulations combined with vertical hydraulic gradient measurements indicate that wave-induced flow recirculations across the groundwater–lake interface are significant. These recirculations, which vary with wave intensity and lake water level fluctuations, set up redox and pH gradients, where Fe precipitates and subsequently sequesters As. The elevated As concentrations observed at both beaches, combined with the distribution of other dissolved species, suggest that the As enrichment may be naturally occurring. Regardless of the As source, the interacting hydrologic and geochemical processes revealed may have important implications for the flux of As and also other oxyanions, such as phosphate, across the groundwater–lake interface in nearshore areas of the Great Lakes.

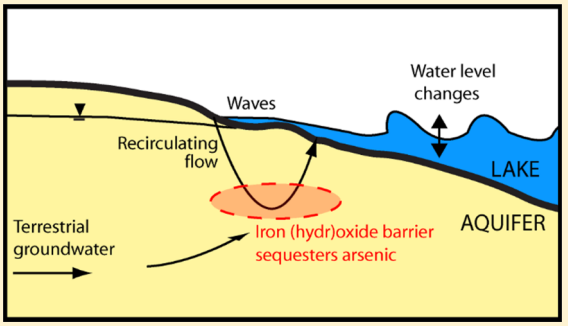

1. INTRODUCTION

The flux of pollutants from groundwater to coastal waters is controlled by the specific pollutant sources, subsurface flow paths, and geochemical processes along these flow paths.[1−3] Along permeable shorelines, coastal water level fluctuations can lead to significant exchange of water and chemicals across the sediment–water interface (SWI).[4−6] The mixing of coastal water recirculating through a nearshore aquifer with terrestrially derived groundwater can set up a reaction zone near the SWI characterized by sharp pH and/or redox gradients.[7−9] Chemicals may undergo transformations in this zone that determine their ultimate fluxes to coastal water.[10,11] Consequently, chemical processing in nearshore aquifers has been shown to influence terrestrial and coastal biogeochemical cycles.[11−13] While this subsurface reaction zone has been well-studied in marine environments (termed a subterranean estuary[14]), its functioning is poorly understood for large inland waters, such as the Great Lakes. The coastal water level fluctuations and the chemical composition of the recirculating coastal water are distinctively different (see section 1 of the Supporting Information).

While the dynamic flows and geochemistry in a nearshore aquifer regulate the flux of many chemical species, this paper focuses on arsenic (As). Arsenic is a highly toxic metalloid, which has attracted enormous attention in environmental studies over the last few decades.[15] Arsenic can occur naturally in aquifers; however, in some cases, its occurrence is attributed to anthropogenic activities, such as mining and industry. The sources and geochemistry of As have been well-studied, e.g., refs 16–18. In recent years, studies have examined the geochemical processes controlling the fate of As in nearshore aquifers and its discharge to coastal water.[19−21] Recent field and numerical investigations[20,19] focused on a marine beach aquifer (Waquoit Bay, MA) demonstrated that the mobility of As near the SWI was controlled by iron (Fe) and manganese (Mn) cycling. Fe (hydr)oxides present where seawater and terrestrial groundwater mix below the SWI acted as a reactive barrier accumulating As. More recently, studies have revealed widespread As enrichment (up to 130 mg/kg) in surface beach sands along the Brazilian coast.[22,23] While sediment analyses indicate that the widespread As enrichment is linked with weathering of a coastal ferruginous sandstone formation marginally enriched in As, the interacting hydrologic and geochemical controls on the mobility of As in the nearshore environment were not explored in that study.

In this paper, we examine the water exchange, groundwater flow, and geochemical processes that control As enrichment in a freshwater beach aquifer. While prior studies (marine and freshwater) generally focused on the geochemistry alone, this

Received: April 24, 2014
Revised: July 29, 2014
Accepted: July 29, 2014
Published: July 29, 2014

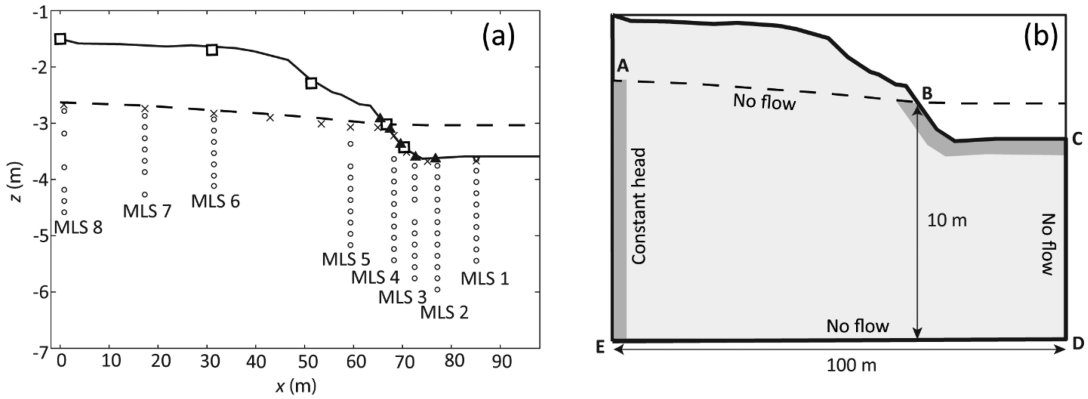

Figure 1. (a) Cross-sectional view of equipment installed at Little Beach along the shore-normal transect on May 14−18, 2012. The solid line in panel a depicts the sand profile, and the dashed line depicts the lake and water table elevations. Manometers (▲) were installed around the shoreline, and piezometers (×) and MLS (○) were installed from the bluff (x = 0 m) to ∼20 m offshore. Five sediment cores (□) were collected in June 2012. (b) Numerical model domain and boundary conditions adopted to simulate groundwater flows at Little Beach. The light shaded region in panel b represents the active model (aquifer) region, and the darker shaded zones along AE and BC depict constant head boundaries.

study also provides insight into the hydrological processes regulating the geochemistry in the beach aquifer. Field data from two Lake Erie beaches are presented. Numerical groundwater flow simulations are used in combination with these data to evaluate the water exchange and groundwater flow patterns that set up the observed geochemical gradients near the shoreline.

2. METHODOLOGY

2.1. Field Sites and Methods. Field measurements were conducted on two nearby beaches (Little Beach and Main Beach) on Lake Erie, Ontario, Canada. These beaches are separated by a creek and a brownfield harbor site (see Figure S2 of the Supporting Information). The east headland of the brownfield site has high groundwater and sediment contamination (e.g., As, Fe, chromium, copper, and lead).[24] Little Beach (∼100 m wide × 180 m long), located adjacent to the east headland, was the focus of the field investigations because there was considerable interest in evaluating the subsurface flux of chemicals from the brownfield site to the lake. Additional field work was conducted at Main Beach (∼600 m long × 85 m wide) to evaluate the pervasiveness of As enrichment in beach aquifers along the shoreline. At both beaches, sediment from the surface to at least 5 m depth is comprised of relatively homogeneous sand and silty sand.

A shore-normal monitoring transect was installed at Little Beach that extended from the base of a glacial till bluff (inland extend of the beach) to 20 m offshore (Figure 1a). Field events were conducted at Little Beach on August 3−5, 2011 and May 14−18, 2012. Two shore-normal transects were also installed at Main Beach: the east transect was located adjacent to the west pier of the brownfield site, and the west transect was located 450 m further west (see Figure S1 of the Supporting Information). The east and west transects were monitored on June 25−28, 2012 and July 30−August 3, 2012, respectively. Long-term lake water level and offshore wave height data are provided in Figure S2 of the Supporting Information.

The equipment layout was similar for all field events (Figure 1a). Piezometers were installed along a shore-normal transect to determine the water table and the lake level elevations. Vertical head gradients around the shoreline were measured using differential manometers connected to nested piezometers (5 mm diameter) with openings at two different depths below the SWI (0.4 and 1.4 m). Water fluxes across the SWI were inferred from these gradient measurements using calculated local hydraulic conductivities (see Table S2 of the Supporting Information). Pore water samples up to 3 m below the sand surface were collected using multi-level samplers (MLS), with sampling ports spaced at 0.2 m depth intervals. Details of the field equipment are provided by Gibbes et al.[25] The location of equipment was surveyed relative to a local permanent benchmark.

2.2. Pore Water Sampling and Analysis. Pore water samples were drawn with syringes from 1.35 mm diameter polyvinyl chloride (PVC) tubes connected to each MLS port. Two samples were collected from each port: 50 mL sample for total As, S, and metal analyses and 60 mL sample for nutrient and dissolved organic carbon (DOC) analyses. Samples for As, S, and metal analyses were stored in 60 mL polyethylene bottles containing 0.5 N nitric acid. Samples for nutrient and DOC analyses were stored in 120 mL glass bottles. All samples were filtered immediately using 0.45 μm nylon filters and frozen until analysis. After sample collection, pore water was pumped into a flow cell and a YSI 6600 Sonde measured physicochemical parameters, including pH and redox potential (Eh).

Total analysis including determination of dissolved As, S, and metals was performed using inductively coupled plasma−optical emission spectroscopy (ICP−OES, Varian, Inc., Vista-Pro Axial). The detection limits for As, Fe, and S were found to be 5 μg/L, 0.001 mg/L, and 0.01 mg/L, respectively, using reference standard solutions (High-Purity Standards ICP-MS-68B Solution A for Fe and As and Fluka Analytica Sulfur Standard for S). Nutrients, including phosphate (PO_4^{3-}), were analyzed using a flow injection nutrient analyzer (Lachat 7500 FIA system), and DOC was analyzed using a total organic carbon (TOC) analyzer (Shimadzu SSM-5000A combustion unit and TOC-Vcpn analyzer). Method blanks were used for all methods, and approximately 5% of the samples were analyzed in duplicate. A check standard was run every 10 samples to check for instrument drift.

2.3. Sediment Cores and Analysis. Five sediment cores (64 mm diameter) up to 1.2 m long were collected at Little Beach in June 2012 using a vibracoring method (Figure 1a and section 4.1 of the Supporting Information). Solid-phase As, Fe, Mn, and Al speciation was estimated on sediment samples

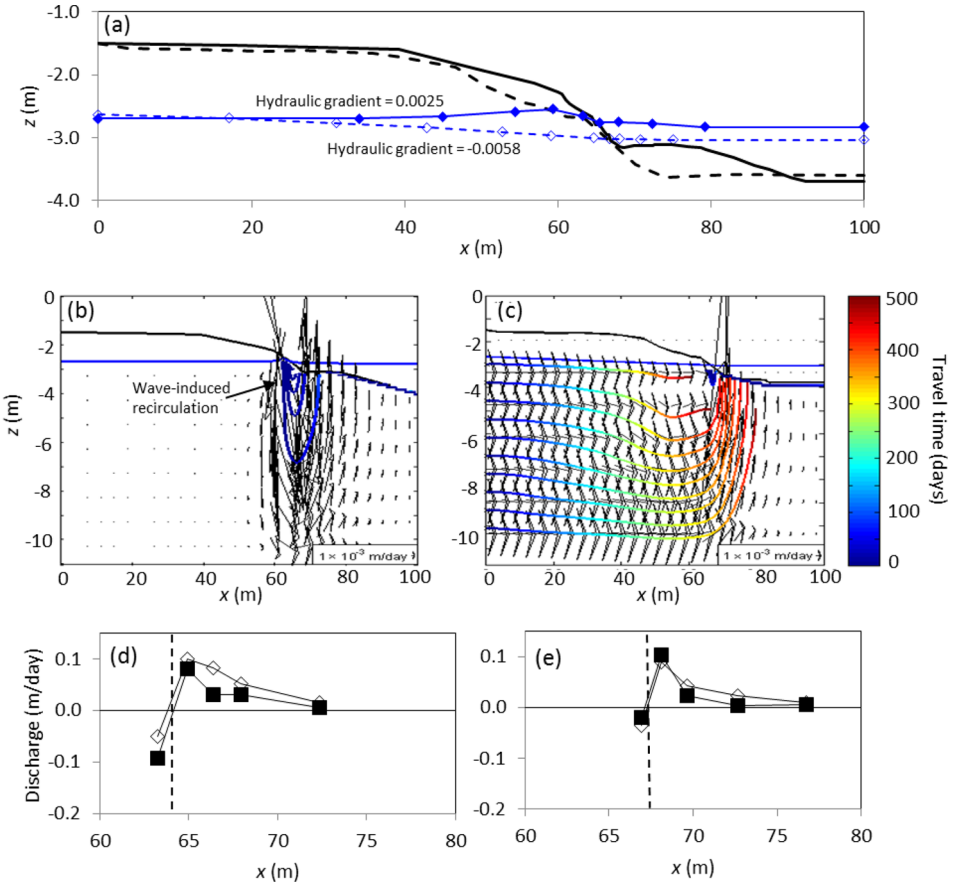

Figure 2. (a) Cross-sectional view of the measured water level and sand level elevations at Little Beach on August 5, 2011 and May 15, 2012. The sand levels (black) and water levels (blue) for August 5, 2011 are depicted by closed diamonds and the solid line. The sand (black) and water levels (blue) for May 15, 2012 are depicted by open diamonds and the dashed line. The corresponding simulated flow velocities (arrows) and particle flow paths are provided for (b) August 5, 2011 and (c) May 15, 2012. The line coloring in panels b and c indicates the travel times (days) for particles as they move along their flow path. The flow paths originating near the wave setup point illustrate the wave-induced flow recirculations. A comparison of the measured (◇) and simulated (■) groundwater discharge rates around the shoreline are shown for (d) August 5, 2011 and (e) May 15, 2012. The dashed vertical line denotes the location of the shoreline. A positive discharge indicates exfiltration to the lake, and a negative discharge indicates infiltration to the aquifer.

using a sequential extraction procedure (SEP) comprised of five main steps, each followed by a wash step. This method, adapted from Wenzel et al.,[26] targets the following extractable fractions: (step 1) SO_4^{2-}, (step 2) $H_2PO_4^{3-}$, (step 3) oxalate, (step 4) ascorbic acid, and (step 5) HNO_3/HCl. These fractions are hereafter nominally ascribed to (step 1) non-specifically bound, (step 2) specifically bound, (step 3) amorphous (hydr)oxide bound, (step 4) crystalline (hydr)oxide bound, and (step 5) residual. SEP method details are provided in section 4.2 of the Supporting Information. Select sediment samples were also analyzed for total S, total C, and organic C (OC) concentrations using the LECO SC444 combustion method.[27]

2.4. Numerical Groundwater Model. Steady-state groundwater flow modeling was conducted using MODFLOW-2005[28] to evaluate the groundwater flow and water exchange patterns during the two field events at Little Beach. Alongshore variability was considered negligible, and therefore, a two-dimensional model was adopted (Figure 1b). The simulated depth of the unconfined aquifer was 10 m. The sediment surface elevation (AC in Figure 1b) was modified to correspond with the surveyed profile for each field event. Specification of the model boundary conditions shown in Figure 1b, including details of the method used to simulate wave effects along BC, is described in section 4.2 of the Supporting Information. Calculated spatially varying hydraulic conductivities were used to parametrize the model domain (see Table S2 of the Supporting Information), and the aquifer was assumed to be isotropic with effective porosity equal to 0.25.

Grid discretization tests were performed to ensure the model had converged. The measured groundwater levels were used to set the starting heads for each simulation. Advective flow paths and transit times were calculated based on the simulated steady-state flows using a conservative particle-tracking algorithm implemented in MATLAB. Particles representing terrestrially derived groundwater were released along a vertical line at $x = 0$ m, and particles representing lake water were released along the submerged SWI at 0.2 m interval.

3. RESULTS AND DISCUSSION

3.1. Groundwater Flows and Water Exchange Rates at Little Beach. Field measurements were combined with groundwater flow modeling to evaluate the groundwater flow and water exchange patterns at Little Beach; understanding of the hydrologic processes provides a basis for interpreting the complex geochemistry observed near the SWI. The water exchange rates and groundwater flows were controlled by the elevation of the inland water table relative to the lake and the wave conditions. A positive hydraulic gradient across the beach

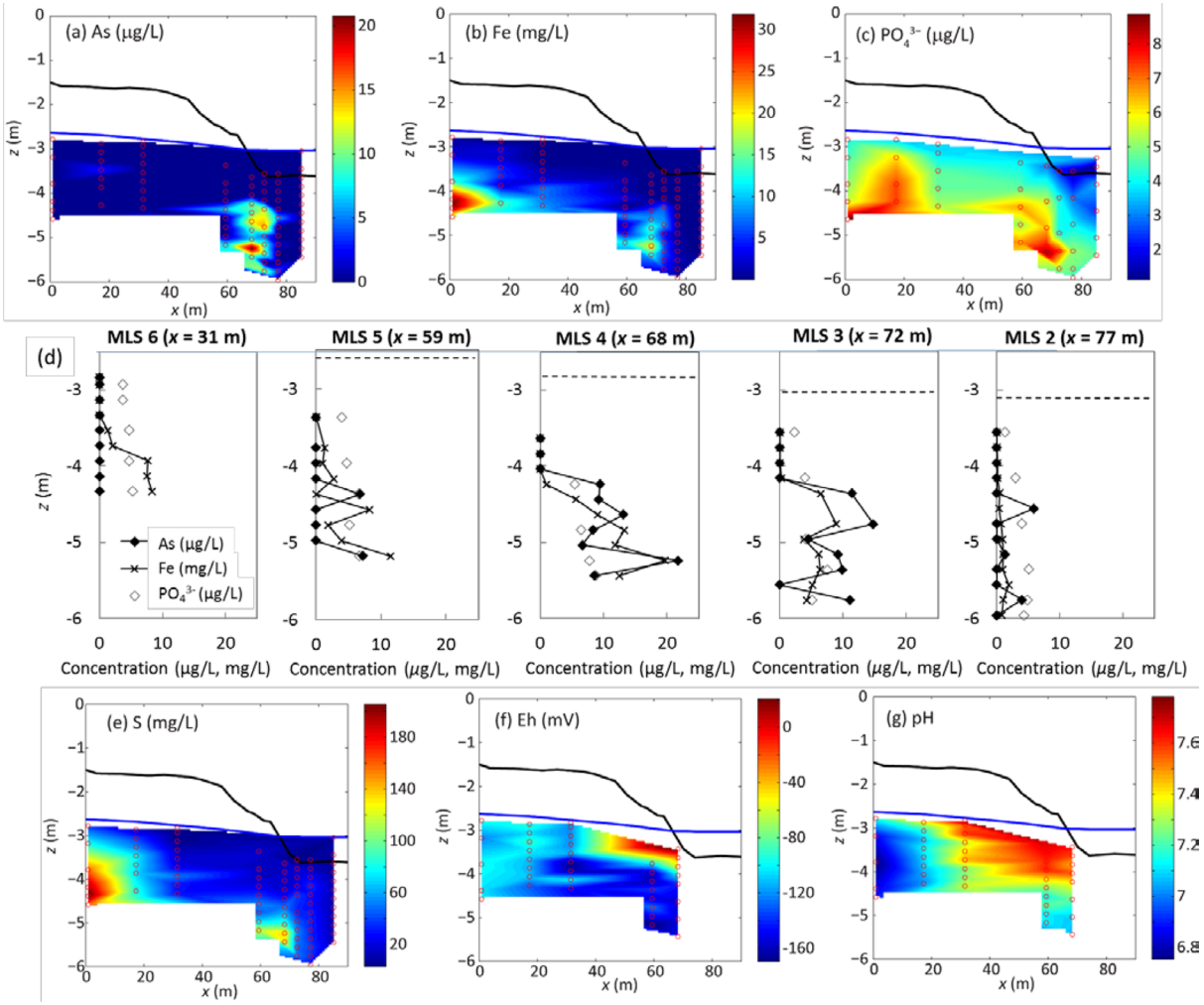

Figure 3. Distributions of dissolved (a) As (μg/L), (b) Fe (mg/L), (c) PO_4^{3-} (μg/L), (e) S (mg/L), (f) Eh, and (g) pH at Little Beach for the May 2012 field event. Corresponding dissolved As (◆), Fe (×), and PO_4^{3-} (○) vertical concentration profiles for MLS installed close to the shoreline (MLS 2–6) are shown in panel d. In contour plots, MLS ports are depicted by the red circles, the solid black line depicts the sand profile (SWI), and the solid blue line depicts the lake and water table elevations. Note the different color scales used for the concentration contour subplots. In panel d, the dashed horizontal lines depict the SWI elevation.

(0.0025), indicating landward groundwater flow, was observed on August 5, 2011, with the water level at the shoreline slightly elevated relative to the inland water table (Figure 2a). In contrast, the hydraulic gradient was −0.0058, and the overall flow direction was lakeward on May 15, 2012 (Figure 2a).

During both field events, the onshore hydraulic gradient associated with wave setup caused lake water to recirculate across the SWI from the wave setup point (intersection of surface water profile with SWI; see Figure S1 of the Supporting Information) to 3–10 m offshore (x = 62.5–72.2 m on August 5, 2011 and x = 65–68 m for May 15, 2012). The simulated wave-induced flow recirculations were wider and deeper on August 5, 2011 compared to May 15, 2012 (panels b and c of Figure 2). This is consistent with past observations[4] of weaker wave-induced recirculations when the lakeward flow is higher, because the discharging groundwater restricts wave-induced infiltration. The simulated water exchange rates around the shoreline compare well to the manometer data for both days, with infiltration close to the wave setup point and exfiltration decreasing offshore (panels d and e of Figure 2). This indicates that the steady-state modeling approach adopted correctly simulates the water exchange around the shoreline in response to the prevailing wave conditions and inland hydraulic gradient.

Particle tracking revealed that, although the steady-state recirculation flow paths are deep, particularly for August 5, 2011 simulation, the average recirculation time was 25 days for August 5, 2011 and 24 days for May 15, 2012. The wave conditions vary continuously, and therefore, infiltrating water would not penetrate to this depth before the wave intensity (and setup) diminished.[29] For August 5, 2011, the simulated infiltration of lake water into the aquifer was 0.73 m^3/day per unit width of aquifer compared to only 0.08 m^3/day for May 15, 2012. Despite the landward flow, the total groundwater discharge rate was also greater for the August 5, 2011 simulation (0.72 m^3/day cf. 0.46 m^3/day) because of the increased wave-induced infiltration.

For the May 15, 2012 simulation, land-derived particles were first transported horizontally before migrating downward around the wave-induced recirculations and discharging slightly offshore (Figure 2c). Because of the low hydraulic gradient, the average time for the particles to discharge through the aquifer was 464 days. In reality, this travel time will vary in response to

dx.doi.org/10.1021/es5020136 | Environ. Sci. Technol. 2014, 48, 10174–10181

time-varying lake and water table elevations and wave conditions.

3.2. Aqueous- and Solid-Phase Geochemistry at Little Beach. Dissolved As was elevated in the groundwater below the shoreline (x = 68−77 m) at Little Beach during the August 2011 and May 2012 field events with observed maximum concentrations of 33 and 22 μg/L, respectively. The distributions of select dissolved species, including As, are shown in Figure S3 of the Supporting Information for August 2011 and in Figure 3 with supplementary data in Figure S4 of the Supporting Information for May 2012. The dissolved As levels found below the shoreline were greater than maximum concentrations historically recorded at the adjacent brownfield site (20 μg/L).[24] The concentrations also exceeded provincial water quality standards for non-potable groundwater (19 μg/L) and industrial background site conditions (13 μg/L).[30]

During the May 2012 field event, As was elevated 1.4−2.4 m below the SWI around the shoreline (MLS 3−5) and sharply declined at a shallower depth with concentrations below detection at ∼1 m depth. Inland (MLS 6−8) and offshore (MLS 1), As concentrations were mostly below detection. The vertical profiles of dissolved As near the shoreline (MLS 3−5) match well with the dissolved Fe profiles; maxima for both elements occurred at z = −5.24 m at MLS 4 (panels a, b, and d of Figure 3). The dissolved As/Fe ratio (μg/mg) mostly ranged between 0.6 and 1.7 at MLS 3−5; this is slightly lower but consistent with dissolved As/Fe ratios reported by Bone et al.[20] for a marine coastal aquifer. The similarity between As and Fe did not hold inland: maximum dissolved Fe (32 mg/L) occurred at MLS 8, and Fe above 8 mg/L was observed along the base of the sampling zone (z < −4 m). Despite this discontinuity, the correlation between Fe and As at MLS 3−5 suggests that As mobility was closely coupled to Fe redox cycling near the shoreline.

The pore water became less reducing (Eh > −100 mV) and had a higher pH (7.5−7.8) at a shallow depth around the shoreline (panels f and g of Figure 3). The increasing pH and Eh above z = −4.24 m at MLS 4 coincided with a sharp decrease in dissolved Fe, indicating that Fe (hydr)oxides may be precipitating as the measured Eh and pH cross the Fe(II)/Fe(III) redox boundary.[31] The oxidation state of As was not measured, but thermodynamic calculations suggest that As(V) should become the dominant As species as pH and Eh increase.[16] At near-neutral pH, As(V) and As(III) have a similar tendency to adsorb to Fe (hydr)oxides surface sites.[32,33] Adsorption of As to precipitated Fe (hydr)oxides likely caused the simultaneous decrease of dissolved As and Fe with depth. PO_4^{3-} also behaves similarly to As(V) at near-neutral pH with a strong affinity to adsorb to Fe (hydr)oxides.[34,35] Consistent with As and Fe, PO_4^{3-} concentrations decreased (although less sharply) at shallower depth near the shoreline (MLS 3 and 4; panels c and d of Figure 3). These trends suggest that Fe precipitation may also be sequestering PO_4^{3-} in the sediment below the shoreline. However, PO_4^{3-} mobility is likely decoupled from that of As because of its cycling during biomass growth and decay.

When the simulated groundwater flows (panels b and c of Figure 2) and aqueous-phase distributions (Figure 3) are compared, it is evident that the wave-induced recirculation of lake water (average pH 7.8 and Eh = 60 mV) may be responsible for the high pH and Eh observed in the pore water around the shoreline and the subsequent redox and pH transitions that control the stability of Fe (hydr)oxides and associated As in the solid phase. While the recirculations deliver oxic lake water to the nearshore sediments, in many freshwater environments, infiltrating surface water also delivers high quantities of DOC, an electron donor.[36] DOC inputs trigger oxygen depletion, and the onset of reducing conditions that follows can favor the reduction of Fe (hydr)oxides and release of As.[16] However, measurements indicate that DOC was spatially heterogeneous, with higher DOC levels observed at the most inland MLS (x = 0 m; 14.2 mg/L) compared to the lake water (2.8 mg/L; see Figure S4 of the Supporting Information). This suggests that the recirculation of lake water with high DO (>8 mg/L) and low DOC relative to the groundwater end member led to more oxic conditions below the shoreline. The zone of high Eh around the shoreline was shallower than the zone of elevated pH because oxygen consumption by available electron donors, such as DOC and Fe^{2+}, is likely faster than water recirculation along the subsurface flow path, which is the main control on pH. The zone of high pH also extended inland of the wave-induced recirculations; this may be due to prior landward groundwater flow that may have transported high pH lake water further inland, i.e., as occurred on August 15, 2011 (Figure 2b).

Results of SEP performed on sediment cores support the aqueous-phase analysis and provide further insight into the solid-phase partitioning of As. While very low As concentrations were released in step 1 (nominally ascribed to non-specifically bound As) for all samples (up to 15 μg/kg; see Table S4 of the Supporting Information), higher concentrations were released in step 2, which targets specifically bound As (ranging from 210 to 580 μg/kg). Notably, the shallowest sample from the core near the shoreline (x = 68 m; z = −3.1 m) had the highest As released in step 2 (Figure 4 and Table S4 of the Supporting Information). This sample also had the highest As released in step 3 (As = 2100 μg/kg), which targets amorphous-oxide-bound species.[37−40] The step 2 and 3 fractions are disproportionately important (increasingly from step 2 to 3) because they can be readily mobilized by environmental changes, such as pH, redox, and available

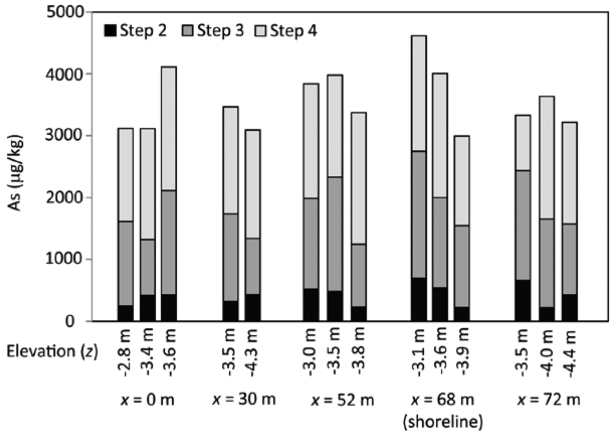

Figure 4. Arsenic solid-phase concentrations as measured from SEP step 2 (nominally specifically sorbed), step 3 (nominally amorphous (hydr)oxide bound), and step 4 (nominally crystalline hydr(oxide) bound). Step 1 results are not shown because As concentrations are too low (<15 μg/kg). Step 5 results are not shown because this fraction is nominally associated with recalcitrant minerals and not readily available. Additional SEP results are provided in section 8 of the Supporting Information.

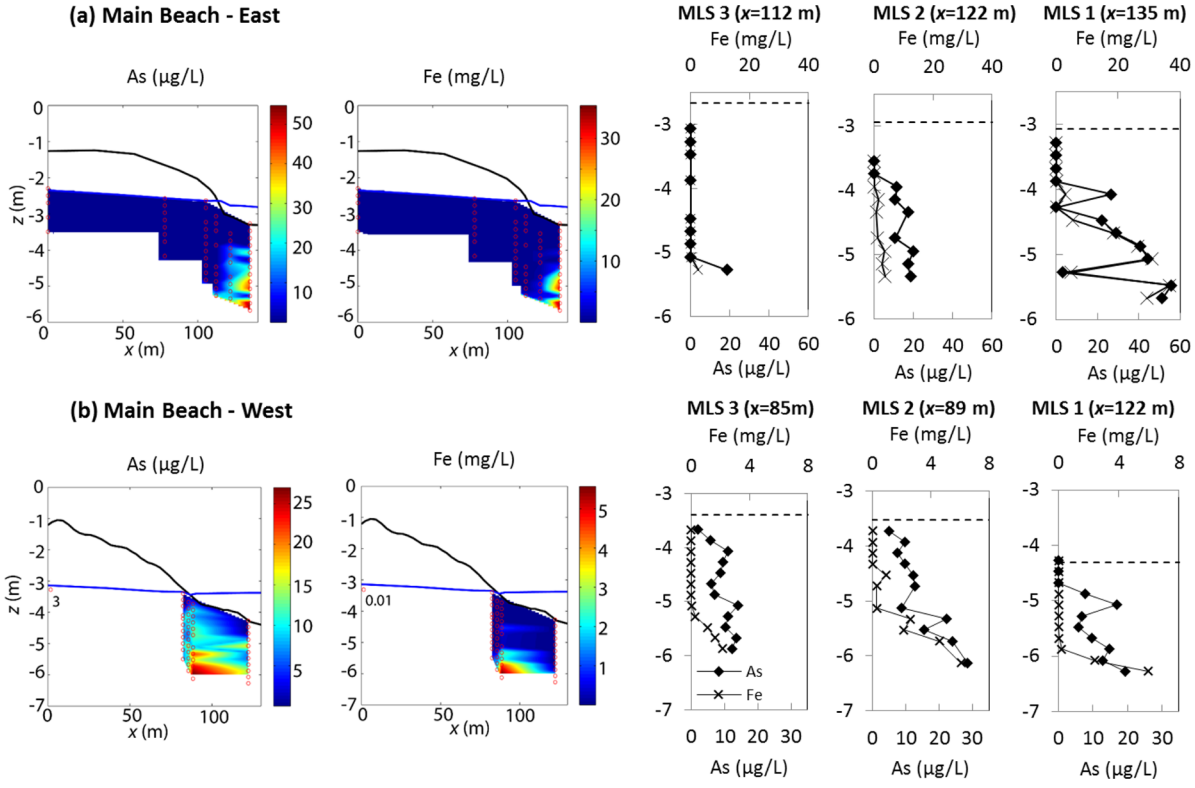

Figure 5. Contoured distributions of dissolved As (μg/L) and Fe (mg/L) concentrations at (a) Main Beach east and (b) Main Beach west transects. The vertical As and Fe concentration profiles for the three lakeward MLS along each transect are also shown. The dashed horizontal lines in the vertical concentration profiles depict the SWI elevation. Note the different color scales used in the concentration contour subplots.

competing ions (e.g., PO_4^{3-}).[37] Arsenic released in steps 2, 3, and 4 accounted for 1−14, 3−47, and 4−63%, respectively, of the total extracted As. Results suggest that Fe (hydr)oxides are considerably more abundant at Little Beach than Mn and Al oxides (see Table S4 of the Supporting Information) and nominally distributed between amorphous (step 3, 722−1910 mg/kg) and crystalline (step 4, 622−3431 mg/kg) phases.

The average ratio of As/Fe in the step 3 fraction was 1.4 (μg/mg) compared to 0.9 (μg/mg) for the step 4 fraction (see Table S4 of the Supporting Information). These ratios are consistent with those previously reported by Bone et al.[20] (average of 0.54 μg/mg), who observed As mobility in a coastal aquifer to be controlled by Fe hydroxide-coated sand. Here, although slightly higher As/Fe ratios were measured for amorphous Fe (hydr)oxides than for crystalline Fe (hydr)-oxides, a better correlation was observed between As and Fe concentrations in crystalline (R^2 = 0.4) than in amorphous (hydr)oxides (R^2 = 0.2; see Figure S5 of the Supporting Information). Together, these observations suggest that Fe amorphous (hydr)oxides play a key role in uptaking As from solution and that As is likely incorporated into the (hydr)oxide phases as they ripen to form more crystalline phases, such as goethite,[5] either as co-precipitates or through irreversible sorption into heterogeneous sites inside the (hydr)oxide aggregate.[6,7] Although high amounts of As and Fe were released in step 5, this residual fraction generally represents As and Fe associated with recalcitrant silicate and As-bearing minerals and is not readily mobile in groundwater.[37,41−44]

Under reducing conditions, As can be immobilized by the precipitation of As sulfide minerals, provided that sufficiently high aqueous As and S concentrations exist or by adsorption onto Fe sulfide minerals.[14] These types of binding however are generally thought to be several orders of magnitude weaker than adsorption onto Fe (hydr)oxides.[6] Thermodynamic calculations suggest that, at Eh > −160 mV and pH of 6.8−7.5 (Figure 3), all S should be in the form of sulfate (SO_4^{2-}) and Fe in the form of ferrous iron (Fe^{2+}). It is therefore unlikely that sulfate reduction and sulfide mineral precipitation occur near the SWI. While high solid-phase S (1100 mg/L) was observed in the shallow sediment near the shoreline (x = 72 m; z = −3.5 m), the OC/S ratio was approximately 17 (see Table S4 of the Supporting Information); this ratio is consistent with that of aquatic microbial biomass rather than sulfide minerals.[13] These results imply that, near the shoreline, As mobility is likely Fe- rather than S-controlled.[15]

The data also suggest that As enrichment below the shoreline is not associated with the same geogenic source that produces elevated dissolved Fe and S in the beach groundwater. While the highest solid-phase S (2900 mg/kg) and residual Fe fraction (3600 mg/kg) were observed for a sediment sample obtained at x = 0 m and z = −3.6 m (see Table S4 of the Supporting Information), both dissolved and solid-phase As were low here. The solid-phase OC/S ratio for this sample was significantly lower (0.6) than that observed near the shoreline (∼17), suggesting that the high solid-phase S may be mostly inorganic. In this sample, the ratio of recalcitrant (step 5) Fe/S was 1.24, which is consistent with Fe sulfide minerals (i.e., FeS and FeS_2). High dissolved Fe and S also found at x = 0 m (MLS 1; panels b and e of Figure 3) further indicate that high dissolved Fe and S in the beach aquifer may be due to Fe sulfide oxidative dissolution.

3.3. Aqueous-Phase Geochemistry at Main Beach. Pore water sampling conducted along the two Main Beach transects found, similar to Little Beach, high dissolved As

dx.doi.org/10.1021/es5020136 | Environ. Sci. Technol. 2014, 48, 10174−10181

concentrations below the SWI with maximum As concentrations of 56 and 29 μg/L at the east and west transects, respectively (Figure 5). At both transects, elevated dissolved As was observed approximately 5−10 m offshore, with concentrations sharply decreasing at shallower depth (e.g., $z = -3.8$ m at MLS 1 and 2; east transect). In comparison to Little Beach, dissolved Fe concentrations were lower inland and only elevated (>5 mg/L) offshore at the Main Beach transects. The As and Fe vertical concentration profiles show similar trends near the shoreline at both transects. The profiles are dissimilar at MLS 1 (offshore) at the west transect. This is likely due to the low Fe concentrations observed here (<5 mg/L); therefore, other species may regulate the As distribution (Figure 5). The pH of the groundwater end member was higher at the Main Beach transects (pH 8.3−9) compared to Little Beach (6.8), and dissolved S in the beach groundwater was also lower (maximum S of 18 and 42 mg/L at the west and east transects, respectively, compared to 209 mg/L at Little Beach; see Figures S9 and S10 of the Supporting Information). The higher pH and lower dissolved Fe and S inland indicate that oxidative dissolution of Fe sulfide minerals may not be significant at these Main Beach sites.

4. SOURCE OF AS IN BEACH GROUNDWATER AND IMPLICATIONS

While leaching of As from the brownfield site with subsequent trapping by Fe (hyr)oxides near the shoreline could explain the As enrichment at Little Beach, it does not explain the elevated As also observed at the Main Beach sites; these site are not directly hydraulically connected with the east headland of the brownfield site. The acidity and high dissolved Fe and S observed at the inland MLS and along the base of the sampling zone at Little Beach suggest that Fe sulfide mineral dissolution may deliver Fe and S to the beach aquifer. Unlike Fe and S, elevated aqueous- and solid-phase As concentrations were not observed inland, indicating that As enrichment below the shoreline is not associated with inland geogenic Fe sulfide deposits. This is further supported by the aqueous-phase geochemistry at Main Beach, where elevated As was still enriched below the shoreline, despite no evidence of inland Fe sulfide deposits.

The lake water contains trace concentrations of As; a lake-wide survey found mean As concentrations of 0.42 μg/L in Lake Erie.[45] Waves and lake water level variations cause relatively high volumes of lake water to recirculate through the aquifer near the shoreline (e.g., 0.73 m^3/day of influx per meter of shoreline estimated for August 15, 2011; Figure 2b). It is possible that As in the recirculating lake water may be sequestered and enriched by adsorption onto Fe (hydr)oxides that precipitate along the redox and pH transition zones. A further study is required to determine the regional extent of the As enrichment in beach groundwater along the shores of the Great Lakes. If this naturally occurring process is widespread, it may have important implications for As contamination levels in nearshore areas of the Great Lakes and other similar freshwater environments.

To our knowledge, this study is the first to demonstrate that, as can occur in marine beaches[20,46] and offshore lake sediments,[47,48] an Fe (hydr)oxide barrier may form below the SWI at freshwater shorelines, which controls the discharge of chemical species that strongly adsorb to these minerals. In contrast to offshore sediments, where As enrichment occurs at millimeter to centimeter depths because transport across the SWI is diffusion-dominated,[47−49] As enrichment in the beach aquifer occurred at much greater depth (meter scale) because of wave-induced advective flows. While this study focused on As, other anionic species, such as PO_4^{3-}, are known to strongly adsorb to Fe (hydr)oxides and may also accumulate. With elevated PO_4^{3-} fluxes to inland waters often implicated in eutrophication, the role of Fe hydr(oxides) in sequestering PO_4^{3-} below the shoreline warrants further investigation. The risk of accumulated species being remobilized and subsequently discharged to nearshore waters remains unclear. Release of As and other adsorbed species may be triggered, for example, by hydraulic changes induced by seasonal lake water level fluctuations or an episodic wave event or, alternatively, by pulses of DOC inputs[49] (e.g., because of algae buildup at the shoreline).

■ ASSOCIATED CONTENT

Supporting Information

Details on the field site locations, numerical model development, and supplementary pore water and solid-phase chemistry data. This material is available free of charge via the Internet at http://pubs.acs.org.

■ AUTHOR INFORMATION

Corresponding Author

*E-mail: crobinson@eng.uwo.ca.

Notes

The authors declare no competing financial interest.

■ ACKNOWLEDGMENTS

This research was supported by Lake Huron & Elgin Area Primary Water Supply Systems, Ontario Ministry of Research and Innovation Early Researcher Award, and a Natural Sciences and Engineering Research Council of Canada (NSERC) Discovery Grant.

■ REFERENCES

(1) Robinson, C.; Brovelli, A.; Barry, D. A.; Li, L. Tidal influence on BTEX biodegradation in sandy coastal aquifers. *Adv. Water Resour.* **2009**, *32* (1), 16−28.

(2) Westbrook, S. J.; Rayner, J. L.; Davis, G. B.; Clement, T. P.; Bjerg, P. L.; Fisher, S. J. Interaction between shallow groundwater, saline surface water and contaminant discharge at a seasonally and tidally forced estuarine boundary. *J. Hydrol.* **2005**, *302* (1−4), 255−269.

(3) Bowen, J. L.; Kroeger, K. D.; Tomasky, G.; Pabich, W. J.; Cole, M. L.; Carmichael, R. H.; Valiela, I. A review of land−sea coupling by groundwater discharge of nitrogen to New England estuaries: Mechanisms and effects. *Appl. Geochem.* **2007**, *22*, 175−191.

(4) Xin, P.; Robinson, C.; Li, L.; Barry, D. A.; Bakhtyar, R. Effects of wave forcing on a subterranean estuary. *Water Resour. Res.* **2010**, *46* (12), W12505.

(5) Robinson, C.; Li, L.; Prommer, H. Tide-induced recirculation across the aquifer−ocean interface. *Water Resour. Res.* **2007**, *43*, W07428.

(6) Santos, I. R.; Eyre, B. D.; Huettel, M. The driving forces of porewater and groundwater flow in permeable coastal sediments: A review. *Estuarine, Coastal Shelf Sci.* **2012**, *98*, 1−15.

(7) Spiteri, C.; Regnier, P.; Slomp, C. P.; Charette, M. A. pH-dependent iron oxide precipitation in a subterranean estuary. *J. Geochem. Explor.* **2005**, *88* (1−3), 399−403.

(8) Ullman, W. J.; Chang, B.; Miller, D. C.; Madsen, J. A. Groundwater mixing, nutrient diagenesis, and discharges across a sandy beachface, Cape Henlopen, Delaware (USA). *Estuarine, Coastal Shelf Sci.* **2003**, *57*, 539−552.

(9) Robinson, C.; Gibbes, B.; Carey, H.; Li, L. Salt−freshwater dynamics in a subterranean estuary over a spring-neap tidal cycle. *J. Geophys. Res.* **2007**, *112* (C9), C09007.
(10) Charette, M. A.; Sholkovitz, E. R. Trace element cycling in a subterranean estuary: Part 2. Geochemistry of the pore water. *Geochem. Cosmochim. Acta* **2006**, *70*, 811−826.
(11) Beck, A. J.; Tsukamoto, Y.; Tovar-Sanchez, A.; Huerta-Diaz, M.; Bokuniewicz, H. J.; Sanudo-Wilhelmy, S. A. Importance of geochemical transformations in determining submarine groundwater discharge-derived trace metal and nutrient fluxes. *Appl. Geochem.* **2007**, *22* (2), 477−490.
(12) Charbonnier, C.; Anschut, P.; Poirier, D.; Bujan, S.; Lecroart, P. Aerobic respiration in a high-energy sandy beach. *Mar. Chem.* **2013**, *155*, 10−21.
(13) Kroeger, K. D.; Charette, M. A. Nitrogen biogeochemistry of submarine groundwater discharge. *Limnol. Oceanogr.* **2008**, *53* (3), 1025−1039.
(14) Moore, W. S. The subterranean estuary: A reaction zone of ground water and sea water. *Mar. Chem.* **1999**, *65* (1−2), 111−125.
(15) Smedley, P. L.; Kinniburgh, D. G. A review of the source, behaviour and distribution of arsenic in natural waters. *Appl. Geochem.* **2002**, *17*, 517−568.
(16) Nordstrom, D. K.; Archer, D. G. Arsenic thermodynamic data and environmental geochemistry. In *Arsenic in Groundwater*; Welch, A. H., Stollenwerk, K. G., Eds.; Kluwer: Dordrecht, Netherlands, 2003; pp 2−25.
(17) Welch, A. H.; Westjohn, D. B.; Helsel, D. R.; Wanty, R. B. Arsenic in ground water of the United States: Occurrence and geochemistry. *Groundwater* **2000**, *38*, 589−604.
(18) Wang, S.; Mulligan, C. N. Occurrence of arsenic contamination in Canada: Sources, behavior and distribution. *Sci. Total Environ.* **2006**, *366*, 701−721.
(19) Jung, H. B.; Charette, M. A.; Zheng, Y. Field, laboratory and modeling study of reactive transport in groundwater arsenic in a coastal aquifer. *Environ. Sci. Technol.* **2009**, *43*, 5333−5338.
(20) Bone, S. E.; Gonneea, M. E.; Charette, M. A. Geochemical cycling of arsenic in a coastal aquifer. *Environ. Sci. Technol.* **2006**, *40* (10), 3273−3278.
(21) Johnston, C. J.; Keene, A. F.; Burton, E. D.; Bush, R. T.; Sullivan, L. A.; McElnea, A. E.; Ahern, C. A.; Smith, C. D.; Powell, B.; Hocking, R. Arsenic mobilization in a seawater inundated acid sulfate soil. *Environ. Sci. Technol.* **2010**, *44*, 1968−1973.
(22) Mirlean, N.; Baisch, P.; Travassos, M. P.; Nassar, C. Calcareous algae bioclast contribution to sediment enrichment by arsenic on the Brazilian subtropical coast. *Geo-Mar Lett.* **2011**, *31*, 65−73.
(23) Mirlean, N.; Garcia, F.; Baisch, P.; Quintana, G. C.; Agnes, F. Sandy beaches contaminated by arsenic, a result of nearshore sediment diagenesis and transport (Brazilian coastline). *Estuarine, Coastal Shelf Sci.* **2013**, *135*, 241−247.
(24) CH2M HILL *Phase II Environmental Site Assessment*; CH2M HILL: Meridian, CO, 2009.
(25) Gibbes, B.; Robinson, C.; Li, L.; Lockington, D. Measurement of hydrodynamics and pore water chemistry in intertidal groundwater systems. *J. Coastal Res.* **2007**, *SI 50*, 884−894.
(26) Wenzel, W. W.; Kirchbaumer, N.; Prohaska, T.; Stingeder, G.; Lombic, E.; Adriano, D. C. Arsenic fractionation in soils using an improved sequential extraction procedure. *Anal. Chim. Acta* **2001**, *436*, 309−323.
(27) Nelson, D. W.; Sommers, L. E. *Total Carbon, Organic Carbon, and Organic Matter, Method Using High-Temperature Induction Furnace*; American Society of Agronomy/Soil Science Society of America: Madison, WI, 1982; Section 29-2.2.4, pp 549−552.
(28) Harbaugh, A. W. *MODFLOW-2005, the U.S. Geological Survey Modular Ground-Water Model—The Ground-Water Flow Process*; U.S. Geological Survey: Reston, VA, 2005.
(29) Robinson, C.; Xin, P.; Li, L.; Barry, D. A. Groundwater flow and salt transport in a subterranean estuary driven by intensified wave conditions. *Water Resour. Res.* **2014**, *50*, 1−17.
(30) Ontario Ministry of the Environment and Climate Change. *Soil, Ground Water and Sediment Standards for Use Under Part XV.1 of the Environmental Protection Act*; Ontario Ministry of the Environment and Climate Change: Toronto Ontario, Canada, 2011.
(31) Stumm, W.; Morgan, J. J. *Aquatic Chemistry: Chemical Equilibria and Rates in Natural Waters*, 3rd ed.; John Wiley and Sons: Hoboken, NJ, 1996.
(32) Goldberg, S. Competitive adsorption of arsenate and arsenite on oxides and clay minerals. *Soil Sci. Soc. Am. J.* **2002**, *66*, 143−421.
(33) Dixit, S.; Hering, J. G. Comparison of arsenic(V) and arsenic(III) sorption onto iron oxide minerals: Implications for arsenic mobility. *Environ. Sci. Technol.* **2003**, *37*, 4182−4189.
(34) Manning, B. A.; Goldberg, S. Modeling competitive adsorption of arsenate with phosphate and molybdate on oxide minerals. *Soil Sci. Soc. Am. J.* **1996**, *60*, 121−131.
(35) Gao, Y.; Mucci, A. Individual and competitive adsorption of phosphate and arsenate on goethite in artificial seawater. *Chem. Geol.* **2003**, *199*, 91−109.
(36) Harvey, J. W.; Böhlke, J. K.; Voytek, M. A.; Scott, D.; Tobias, C. R. Hyporheic zone denitrification: Controls on effective reaction depth and contribution to whole-stream mass balance. *Water Resour. Res.* **2013**, *49*, 6298−6316.
(37) Kim, E. J.; Yoo, J.-C.; Baek, K. Arsenic speciation and bioaccessibility in arsenic-contaminated soils: Sequential extraction and mineralogical investigation. *Environ. Pollut.* **2014**, *186*, 29−35.
(38) Yang, L.; Steefel, C. I.; Marcus, M. A.; Bargar, J. R. Kinetics of Fe(II)-catalyzed transformation of 6-line ferrihydrite under anaerobic flow conditions. *Environ. Sci. Technol.* **2010**, *44* (14), 5469−5475.
(39) Couture, R. M.; Rose, J.; Kumar, N.; Mitchell, K.; Wallschläger, D.; Van Cappellen, P. Sorption of arsenite, arsenate and thioarsenates to iron oxides and iron sulfides: A kinetic and spectroscopic investigation. *Environ. Sci. Technol.* **2013**, *47* (11), 5652−5659.
(40) Fuller, C. C.; Davis, J. A.; Waychunas, G. A. Surface chemistry of ferrihydrite: Part 2. Kinetics of arsenate adsorption and coprecipitation. *Geochim. Cosmochim. Acta* **1993**, *57* (10), 2271−2282.
(41) Filgueiras, A. V.; Lavilla, I.; Bendicho, C. Chemical sequential extraction for metal partitioning in environmental solid samples. *J. Environ. Monit.* **2002**, *4*, 823−857.
(42) Wolthers, M.; Charlet, L.; van der Weijden, C. H.; van der Linde, P. R.; Rickard, D. Arsenic mobility in the ambient sulfidic environment: Sorption of arsenic(V) and arsenic(III) onto disordered mackinawite. *Geochim. Cosmochim. Acta* **2005**, *69*, 3483−3492.
(43) Fagerbakke, K. M.; Heldal, M.; Norland, S. Content of carbon, nitrogen, oxygen, sulfur and phosphorus in native aquatic and cultured bacteria. *Aquat. Microb. Ecol.* **1996**, *10* (1), 15−27.
(44) O'Day, P. A.; Vlassopoulos, D.; Root, R.; Rivera, N. The influence of sulfur and iron on dissolved arsenic concentrations in the shallow subsurface under changing redox conditions. *Proc. Natl. Acad. Sci. U. S. A.* **2004**, *101*, 13703−13708.
(45) Rossmann, R.; Barres, J. Trace element concentrations in near-surface waters of the Great Lakes and methods of collection, storage and analysis. *J. Great Lakes Res.* **1988**, *14* (2), 188−204.
(46) Charette, M. A.; Sholkovitz, E. R. Oxidative precipitation of groundwater-derived ferrous iron in the subterranean estuary of a coastal bay. *Geophys. Res. Lett.* **2002**, *29* (10), 85-1−85-4.
(47) Toevs, G.; Morra, M. J.; Winowiecki, L.; Strawn, D.; Polizzotto, M. L.; Fendorf, S. Depositional influences on porewater arsenic in sediments of a mining-contaminated freshwater lake. *Environ. Sci. Technol.* **2008**, *42* (18), 6823−6829.
(48) Couture, R. M.; Gobeil, C.; Tessier, A. Arsenic, iron and sulfur co-diagenesis in lake sediments. *Geochem. Cosmochim. Acta* **2010**, *74*, 1238−1255.
(49) Martin, A. J.; Pedersen, T. F. Seasonal and interannual mobility of arsenic in a lake impacted by metal mining. *Environ. Sci. Technol.* **2002**, *36*, 1516−1523.